

## A theory for self-diffusion in liquids

Maxim Vergeles and Grzegorz Szamel

Chemistry Department, Colorado State University, Fort Collins, Colorado 80523

(Received 13 October 1998; accepted 3 November 1998)

We propose an alternative approach to self-diffusion in an atomic liquid. Our starting point is an oscillatory motion of a tagged particle in its first solvation shell (cage). Only after cage relaxation is taken into account is the tagged particle able to diffuse. This approach is suitable for describing liquids where the concept of binary collisions breaks down and the self-diffusion coefficient is small. Our predictions quantitatively agree with the results of MD simulations in a broad range of densities and temperatures up to the freezing transition. © 1999 American Institute of Physics. [S0021-9606(99)50606-5]

### I. INTRODUCTION

A variety of chemically important processes in liquids involve dynamical behavior of a single molecule in a solvent. The simplest one (and perhaps the least chemically relevant) is self-diffusion. Other examples include dynamics of solvation,<sup>1,2</sup> vibrational relaxation,<sup>3,4</sup> and quadrupolar relaxation.<sup>5</sup> In spite of the conceptual simplicity of these processes, their description is highly nontrivial due to coupling of the single-molecule degrees of freedom to all the solvent dynamical degrees of freedom.

Here we present a theory for single-molecule processes in liquids. We apply this theory to self-diffusion in an atomic liquid mainly because it is the most familiar process, but also because it is the most extensively studied one.

Conceptually, most of the current theories of self-diffusion in liquids originate from the Boltzmann equation. The underlying paradigm of these theories is understanding the dynamics through analysis of sequences of binary collisions.<sup>6</sup> The simplest class of binary collisions, so-called independent binary collisions, is fully accounted for by the Boltzmann theory. The major achievement of the “modern era” of kinetic theory was the understanding of the importance of dynamically correlated collisions.<sup>6,7</sup>

The binary collision picture is applicable at low to moderate densities.<sup>8,9</sup> However, as the density increases its validity becomes questionable. To justify the use of binary collisions one needs a separation of time scales: the duration of an average collision, the collision time, should be much shorter than the average time between successive collisions, the mean free time. Figure 1 compares the time dependence of the velocity autocorrelation function (VACF),

$$C_v(t) = \frac{\langle \mathbf{v}_1(t) \cdot \mathbf{v}_1(0) \rangle_{\text{eq}}}{\langle \mathbf{v}_1 \cdot \mathbf{v}_1 \rangle_{\text{eq}}}, \quad (1)$$

with that of two different (normalized) force correlation functions (all dimensional quantities in this paper are given in MD units, see Appendix C). VACF decays on the time scale of the mean free time and the force correlation functions decay on the time scale of the mean collision time. The first force correlation function is the autocorrelation function of the total force acting on the tagged particle (FACF),

$$G_F(t) = \left\langle \sum_{i \neq 1} \mathbf{F}_{1i}(t) \cdot \sum_{i \neq 1} \mathbf{F}_{1i}(0) \right\rangle_{\text{eq}} \equiv G_F(t=0) \times C_F(t). \quad (2)$$

The second one is the “binary” contribution to the FACF or, in other words, the autocorrelation function of the force on the tagged particle that is due to one specific other particle (sFACF),

$$G_F^s(t) = \left\langle \sum_{i \neq 1} \mathbf{F}_{1i}(t) \cdot \mathbf{F}_{1i}(0) \right\rangle_{\text{eq}} \equiv G_F^s(t=0) \times C_F^s(t). \quad (3)$$

Strictly speaking, for the binary collision picture to be valid the normalized force correlation functions  $C_F$  and  $C_F^s$  should decay much faster than VACF and the un-normalized functions  $G_F$  and  $G_F^s$  should be (approximately) equal. It is clear from Fig. 1 that the first condition is violated at liquid densities. The mean free time and the collision time, quite different at low densities, become comparable at liquid densities. In addition, Fig. 2 shows that the magnitude of the two un-normalized force correlation functions is very different at liquid densities. Thus the (total) force acting on the tagged particle originates from all the neighboring particles or from the solvation shell of the tagged particle. These two facts, in our opinion, make the binary collision picture generally invalid at liquid densities.

Interestingly, there is one system for which the above conclusion does not apply. In a system of hard spheres, collisions are always instantaneous. Therefore the binary collision picture is valid at any density. That perhaps explains the remarkable success of Enskog’s theory in predicting dynamical properties of hard-sphere fluids. Enskog’s theory includes only independent binary collisions; however, it does take into account a modification of the collision frequency due to static correlations. With regard to self-diffusion, Enskog’s theory misses two important effects:<sup>7</sup> the long-time tail (“vortex diffusion”) and the negative region in the VACF (“cage diffusion”). These two effects originate from dynamically correlated collisions.<sup>7</sup> An advanced kinetic-theory-type analysis<sup>10,11</sup> and a mode-mode coupling approach<sup>12</sup> were used to include the correlated collisions. The resulting

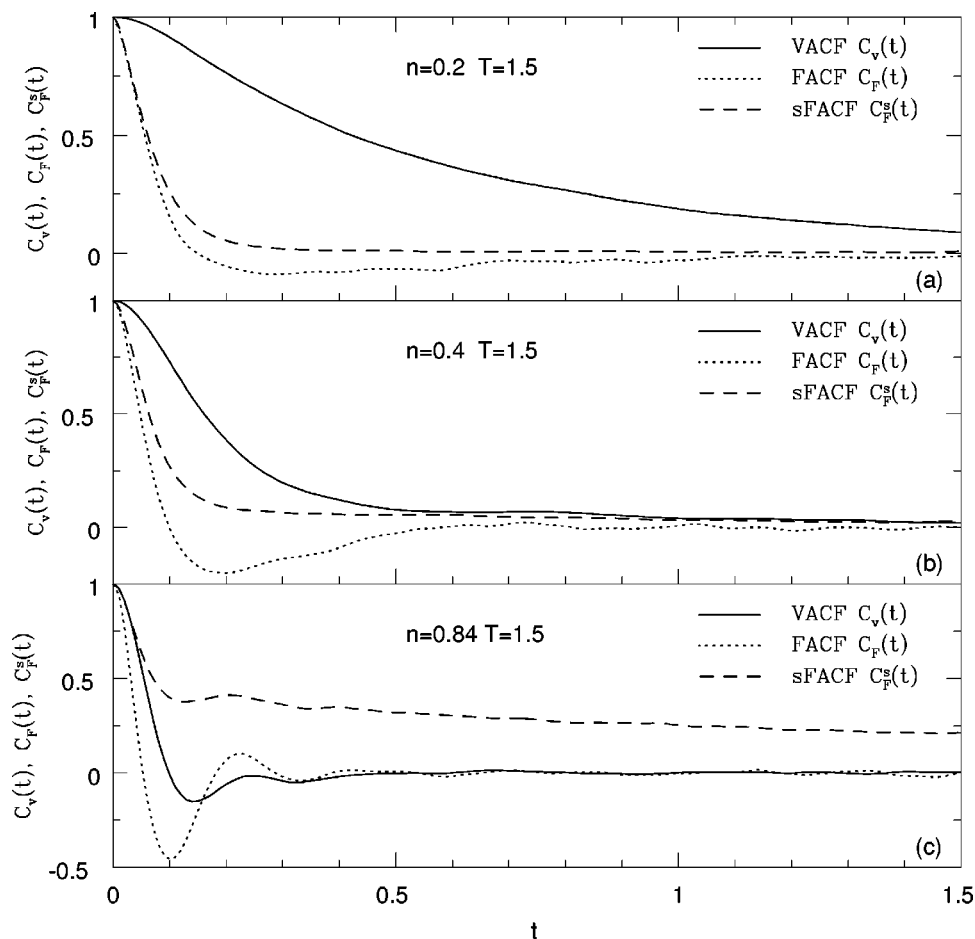


FIG. 1. VACF  $C_v$  (solid lines), and normalized force autocorrelation functions,  $C_F$  (dotted lines) and  $C_F^s$  (dashed lines), at  $T=1.5$  and  $n=0.2$  (a),  $n=0.4$  (b) and  $n=0.84$  (c). The data were obtained from MD simulations of 1372 particles of mass  $m$ , interacting via a pairwise potential  $V(r)=4\epsilon(\sigma/r)^{12}$ . Temperature is measured in  $\epsilon/k_B$ , density is measured in  $\sigma^{-3}$  and time is measured in  $\tau=\sigma\sqrt{m/\epsilon}$ .

density dependence of the self-diffusion coefficient and VACF agrees well with molecular dynamics simulations of the hard-sphere system.<sup>13</sup>

As has been argued above, the binary collision picture is not applicable to dense liquids with continuous interactions. In spite of this fundamental difficulty, a hard-sphere-inspired analysis has been used in this case too. However, in practical applications<sup>14</sup> the short-time dynamics, that is the independent binary collision dynamics in the hard sphere case, has to be assumed to be different from the binary collision dynamics. Had this not been done the theory would have greatly overestimated the magnitude of the second time derivative of VACF at short times. In Ref. 14 a phenomenological Gaussian form (involving *many-particle dynamics*) was used for the short-time part of the memory function. A concept of renormalized (or “hard”) binary collisions is often invoked to justify this procedure. However, these renormalized collisions have never been explicitly derived from the underlying microscopic dynamics.

Another, related difference between dynamics of hard sphere fluids and dynamics of liquids with continuous interactions should be mentioned here. In the hard sphere case independent binary collisions lead to a monotonically decaying VACF. “Cage diffusion” has to be invoked in order to describe the negative region in the VACF. For fluids with continuous interactions independent binary collisions lead to a VACF that shows damped oscillations. Qualitatively the same result is obtained if renormalized or “hard” collisions

are used. To the best of our knowledge this fact was first reported 25 years ago in a short paper by Kim and Chandler.<sup>15</sup>

An approach that is conceptually very different from kinetic theory was initiated by Zwanzig.<sup>16</sup> He suggested that one should start from a disordered-solid-like picture of a liquid, i.e., oscillations about a local minimum on the potential energy surface. Furthermore, self-diffusion (and other dissipative phenomena) should follow from infrequent “jumps” between different local minima.

Zwanzig’s original idea has been reformulated in several different ways.<sup>17–19</sup> The most popular of these, an instantaneous normal modes (INM) approach,<sup>17</sup> has proven to be extremely useful for analyzing the short-time dynamics of liquids.<sup>2,20</sup> The INM approach has also been extended to self-diffusion.<sup>21</sup> It has been shown to give quantitatively accurate results for the self-diffusion coefficient in a variety of liquids. However, the INM-based theory of self-diffusion has been criticized.<sup>22,23</sup> It seems fair to say that there is no *generally accepted* theory, based on Zwanzig’s idea, that can make predictions for the long-time dynamical properties of liquids using only static (*equilibrium*) input.<sup>19,22</sup>

The theory presented here attempts to combine the tools of kinetic theory with the conceptual picture of Zwanzig. We start with an oscillatory motion of a tagged particle in its first solvation shell. Thus in the zeroth order the self-diffusion coefficient vanishes. In the next order the cage particles are

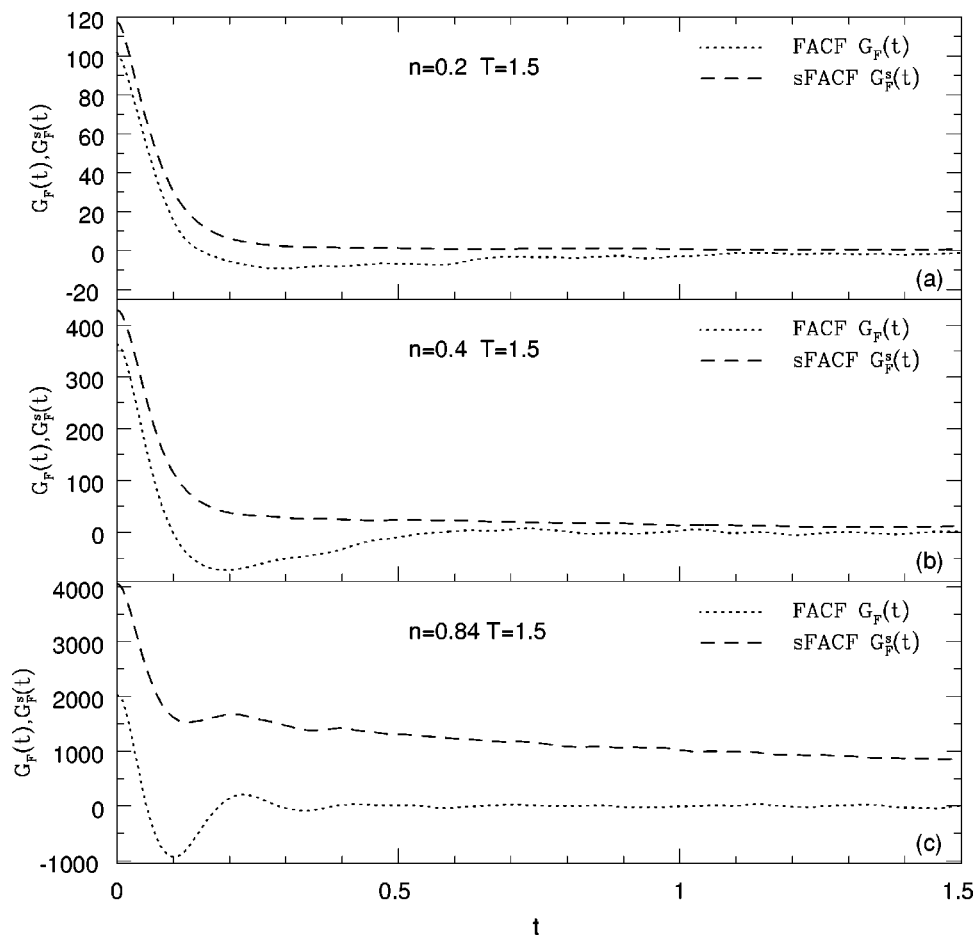


FIG. 2.  $Un$ -normalized force autocorrelation functions,  $G_F$  (dotted lines) and  $G_F^s$  (dashed lines) at  $T=1.5$  and  $n=0.2$  (a),  $n=0.4$  (b) and  $n=0.84$  (c).

allowed to move, making it possible for the tagged particle to diffuse out (and making the self-diffusion coefficient non-zero). This should be contrasted with the binary collision approach, which, in the zeroth order, starts with free streaming and an infinite self-diffusion coefficient. In the next order binary collisions of the tagged particle with other particles are included and that makes the self-diffusion coefficient finite. We expect that at liquid densities, oscillations, with a vanishing self-diffusion coefficient, make a better starting point than free streaming with an infinite self-diffusion coefficient.<sup>24</sup>

In order to implement this program we have chosen to use distribution functions which depend not only on positions and velocities of particles, but also on the total force acting on the tagged particle. Thus, for example, our one-particle (singlet) distribution function describes not only the state of the tagged particle but also the state of the local environment of the tagged particle. The advantage of this nonorthodox definition is that it allows us to derive simple, local in time, evolution equations describing the oscillatory motion of the tagged particle in its first solvation shell.

In the remainder of the paper we will construct the formal theory and apply it to the calculation of the self-diffusion coefficient  $D$ , VACF  $C_v(t)$  and the memory function<sup>25</sup>  $\zeta(t)$ .

## II. THEORETICAL FORMALISM

We consider a simple fluid consisting of particles of unit mass interacting via potential  $V(r)$ . The first particle is tagged but otherwise identical to the other ones. We begin by introducing a set of distribution functions

$$\begin{aligned}
 f_i(\mathbf{r}_1, \mathbf{v}_1, \dots, \mathbf{r}_i, \mathbf{v}_i, \mathbf{F}; t) \\
 = \frac{(N-1)!}{(N-i)!} \int d\Gamma \prod_{k \leq i} \delta(\mathbf{r}_k - \mathbf{R}_k) \\
 \times \delta(\mathbf{v}_k - \mathbf{V}_k) \delta\left(\mathbf{F} - \sum_{j \neq 1} \mathbf{F}_{1j}\right) \rho_N(t),
 \end{aligned} \tag{4}$$

where  $\Gamma$  denotes positions and velocities of all the particles,  $\Gamma \equiv (\mathbf{R}_1, \dots, \mathbf{R}_N; \mathbf{V}_1, \dots, \mathbf{V}_N)$ ,  $\rho_N(t)$  is the time-dependent  $N$ -particle distribution function,  $\mathbf{F}$  is the total force acting on the tagged particle (particle 1),  $\mathbf{F}_{1j} = -\partial V(\mathbf{R}_1 - \mathbf{R}_j) / \partial \mathbf{R}_1$  is the force acting on the tagged particle from the particle  $j$ . Thus  $f_1(\mathbf{r}_1, \mathbf{v}_1, \mathbf{F}; t)$  is the probability that the tagged particle at a time  $t$  is at  $\mathbf{r}_1$ , moves with a velocity  $\mathbf{v}_1$  and experiences a force  $\mathbf{F}$ ,  $f_2(\mathbf{r}_1, \mathbf{v}_1, \mathbf{r}_2, \mathbf{v}_2, \mathbf{F}; t)$  is the probability that at a time  $t$  the tagged particle is at  $\mathbf{r}_1$ , moves with a velocity  $\mathbf{v}_1$  and experiences a force  $\mathbf{F}$  and that another particle is at  $\mathbf{r}_2$  and moves with a velocity  $\mathbf{v}_2$ . Other distributions  $f_i$  ( $i \geq 3$ ) have a similar meaning.

The time evolution of  $f_i$  is described by an infinite hierarchy of equations that is similar to the BBGKY hierarchy<sup>26</sup> known from the kinetic theory. Here we need the first two equations of this hierarchy:

$$\frac{\partial f_1}{\partial t} = -\mathbf{v}_1 \cdot \frac{\partial f_1}{\partial \mathbf{r}_1} - \mathbf{F} \cdot \frac{\partial f_1}{\partial \mathbf{v}_1} + \int d2 \mathbf{B}_{12} \cdot \frac{\partial f_2}{\partial \mathbf{F}}, \quad (5)$$

$$\frac{\partial f_2}{\partial t} = \hat{L}_2 f_2 + \int d3 \mathbf{B}_{13} \cdot \frac{\partial f_3}{\partial \mathbf{F}} + \int d3 \frac{\partial V(\mathbf{r}_{23})}{\partial \mathbf{r}_2} \cdot \frac{\partial f_3}{\partial \mathbf{v}_2}, \quad (6)$$

where  $di \equiv d\mathbf{r}_i d\mathbf{v}_i$  and  $\mathbf{B}_{ij}$ , and  $\hat{L}_2$  are given by:

$$\mathbf{B}_{ij} = \frac{\partial}{\partial \mathbf{r}_i} \left( (\mathbf{v}_i - \mathbf{v}_j) \cdot \frac{\partial V(\mathbf{r}_{ij})}{\partial \mathbf{r}_i} \right), \quad (7)$$

$$\begin{aligned} \hat{L}_2 = & -\mathbf{v}_1 \cdot \frac{\partial}{\partial \mathbf{r}_1} - \mathbf{F} \cdot \frac{\partial}{\partial \mathbf{v}_1} - \mathbf{v}_2 \cdot \frac{\partial}{\partial \mathbf{r}_2} \\ & + \frac{\partial V(\mathbf{r}_{12})}{\partial \mathbf{r}_2} \cdot \frac{\partial}{\partial \mathbf{v}_2} + \mathbf{B}_{12} \cdot \frac{\partial}{\partial \mathbf{F}}. \end{aligned} \quad (8)$$

A brief derivation of the hierarchy (5)–(6) is presented in Appendix A.

We start by rewriting Eqs. (5)–(6) in a way that is analogous to that used in kinetic theory. To this end we introduce  $y_1 = f_1 / f_1^{\text{eq}}$  and  $h_i = f_i - f_i^{\text{eq}} y_1$ , where  $f_i^{\text{eq}}$  represent  $f_i$  at equilibrium. One should note here that  $h_i$  represent dynamical correlations: it can be shown that the approximation consisting in neglecting all of them,  $h_i = 0$ , is equivalent to assuming that the  $N$ -particle probability distribution  $\rho_N$  is equal to the *local equilibrium* distribution  $\rho_N^{\text{leq}}$ , where

$$\rho_N^{\text{leq}}(t) = \rho_N^{\text{eq}} \frac{f_1(t)}{f_1^{\text{eq}}}. \quad (9)$$

The local equilibrium distribution at time  $t$  depends only on the state of the tagged particle at the same time and thus does not include dynamical correlations.

We first rewrite Eq. (5) and obtain

$$\frac{\partial y_1}{\partial t} = \hat{L}_0 y_1 + \frac{1}{f_1^{\text{eq}}} \int d2 \mathbf{B}_{12} \cdot \frac{\partial h_2}{\partial \mathbf{F}}, \quad (10)$$

where

$$\hat{L}_0 = -\mathbf{v}_1 \cdot \frac{\partial}{\partial \mathbf{r}_1} - \mathbf{F} \cdot \frac{\partial}{\partial \mathbf{v}_1} + (\tilde{\Omega}^2 \cdot \mathbf{v}_1) \cdot \frac{\partial}{\partial \mathbf{F}}, \quad (11)$$

$$\tilde{\Omega}^2(\mathbf{F}) = \int d2 \frac{f_2^{\text{eq}}}{f_1^{\text{eq}}} \frac{\partial^2 V(\mathbf{r}_{12})}{\partial \mathbf{r}_1 \partial \mathbf{r}_1}. \quad (12)$$

If the dynamical correlations are neglected,  $h_2 = 0$ , evolution of the tagged particle distribution is described by operator  $\hat{L}_0$ . Equivalently, the tagged particle's dynamics is given by the following equations of motion:

$$\dot{\mathbf{r}}_1 = \mathbf{v}_1, \quad (13a)$$

$$\dot{\mathbf{v}}_1 = \mathbf{F}, \quad (13b)$$

$$\dot{\mathbf{F}} = -\tilde{\Omega}^2(\mathbf{F}) \cdot \mathbf{v}_1. \quad (13c)$$

TABLE I. The second and fourth time derivatives of the VACF as a function of density  $n$  at  $T=1.5$ . The accuracy of all results in the table is about 1%.

$n$	$-\ddot{C}_v(t=0)$	$-\ddot{C}_v(t=0) _{bc}$	$\ddot{C}_v(t=0)$	$\ddot{C}_v(t=0) _{th}$
0.2	24.07	26.22	12732	13609
0.4	76.20	94.87	48521	64626
0.84	446.46	896.00	565095	690529

These equations describe an oscillatory motion of the tagged particle with  $\tilde{\Omega}$ , Eq. (12), playing the role of an *instantaneous* frequency tensor. In other words,  $\tilde{\Omega}$  describes how the force changes when the tagged particle is moving. The force change does depend on the local environment of the tagged particle. Thus the instantaneous frequency  $\tilde{\Omega}$  depends on the force and therefore the oscillations are anharmonic.

It should be noted here that  $\tilde{\Omega}^2$  is, in a sense, analogous to the matrix of second derivatives of the potential energy that is the starting point of the INM approach.<sup>17</sup> The main difference is that  $\tilde{\Omega}^2$  is a *local* quantity. It describes, on average, the shape of the potential energy in the neighborhood of the tagged particle. The second difference is that  $\tilde{\Omega}^2$  depends on  $\mathbf{F}$  and thus changes in time whereas the time dependence of the matrix of second derivatives of the potential energy used in the INM is usually neglected.

Next we rewrite Eq. (6) and obtain

$$\frac{\partial h_2}{\partial t} = \hat{L}_2 h_2 + f_2^{\text{eq}} \mathbf{B}_{12} \cdot \frac{\partial y_1}{\partial \mathbf{F}} + H_3, \quad (14)$$

where

$$\begin{aligned} H_3 = & -\frac{f_2^{\text{eq}}}{f_1^{\text{eq}}} \int d2' \mathbf{B}_{12'} \cdot \frac{\partial h_2(2')}{\partial \mathbf{F}} + \int d3 \mathbf{B}_{13} \cdot \frac{\partial h_3}{\partial \mathbf{F}} \\ & + \int d3 \frac{\partial V_{23}}{\partial \mathbf{r}_2} \cdot \frac{\partial h_3}{\partial \mathbf{v}_2} \\ & + \left( \int d3 f_3^{\text{eq}} \mathbf{B}_{13} - \frac{f_2^{\text{eq}}}{f_1^{\text{eq}}} \int d2' f_2^{\text{eq}}(2') \mathbf{B}_{12'} \right) \cdot \frac{\partial y_1}{\partial \mathbf{F}}. \end{aligned} \quad (15)$$

$H_3$  represents all the *three-particle* terms in Eqs. (10) and (14), i.e., terms involving simultaneous motion of three particles.

It should be emphasized that  $H_3$  includes the three-particle dynamical correlations represented by  $h_3$ . To describe time evolution of these correlations we need the next equation of the hierarchy. It is clear that in order to get a closed system of equations we have to cut the hierarchy.

Our *closure approximation* consists of neglecting the three-particle terms in Eq. (14). This is similar in spirit to the closure approximation used in the binary collision approach.<sup>8,9</sup> Both in the binary collision approach and in our theory the goal is to end up with a two-particle dynamics of some kind. An *a priori* assessment of our closure is difficult

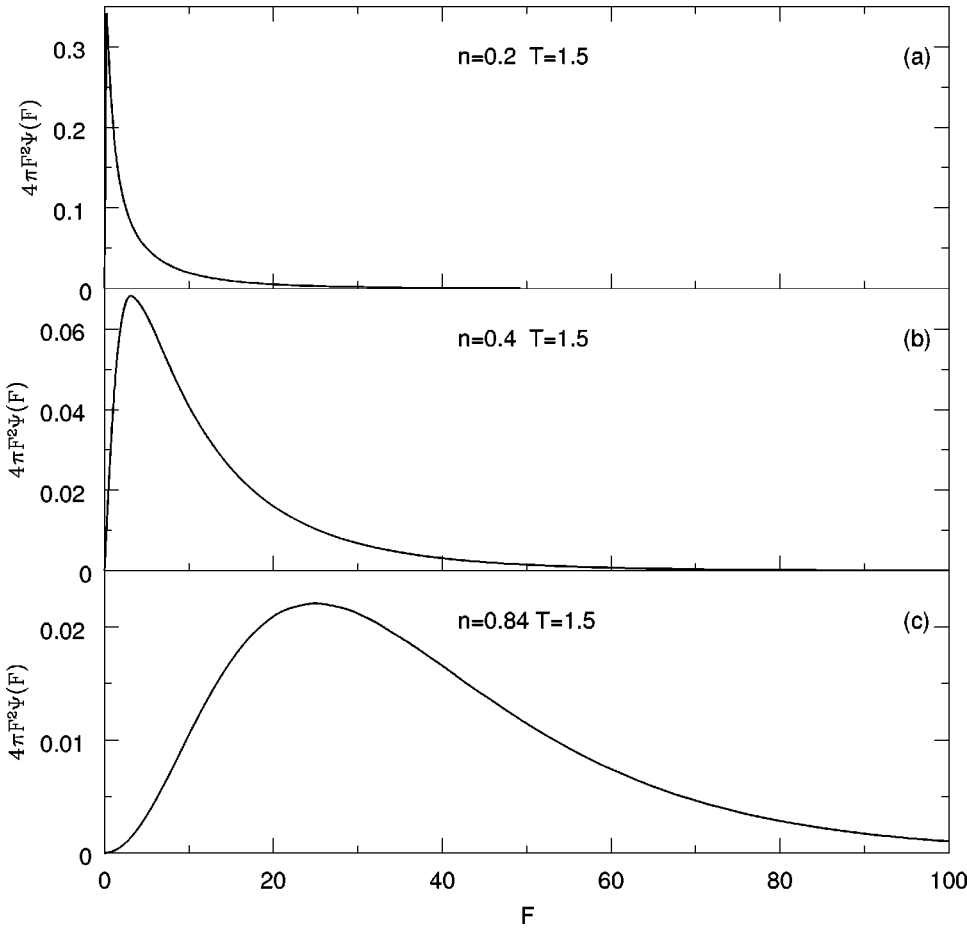


FIG. 3. The equilibrium distribution of the total force acting on the tagged particle at  $T=1.5$  and  $n=0.2$  (a),  $n=0.4$  (b) and  $n=0.84$  (c).

(as usually is the case in kinetic theories), but the accuracy of the approximations made can be estimated by comparing out theoretical predictions with exact results.

After dropping  $H_3$  we are left with a system of two closed equations. We then formally solve Eq. (14) and substitute the solution into Eq. (10). In this way we obtain a single closed equation for  $y_1$ :

$$\frac{\partial y_1}{\partial t} = \hat{L}_0 y_1 + \frac{1}{f_1^{\text{eq}}} \int d2\mathbf{B}_{12} \cdot \frac{\partial}{\partial \mathbf{F}} \times \int_0^t d\tau e^{\hat{L}_2(t-\tau)} f_2^{\text{eq}} \mathbf{B}_{12} \cdot \frac{\partial y_1(\tau)}{\partial \mathbf{F}}. \quad (16)$$

Equation (16) is the main formal result of the present work.

As discussed above, according to Eq. (16), in the zeroth order (i.e., when the integral term at the right-hand-side of Eq. (16) is neglected), the tagged particle performs an (anharmonic) oscillatory motion. The second term can be interpreted as describing an escape of the tagged particle from its original cage, made possible by the motion of the cage particles.

It is worthwhile to contrast Eq. (16) with an analogous equation derived in the framework of the binary collision approach (see, e.g., Eq. (2.2) of Ref. 9). There, in the zeroth order the tagged particle moves freely, and an integral term describes binary collisions of the tagged particle with other particles of the fluid.

### III. VACF: GENERAL CONSIDERATIONS

We use Eq. (16) to calculate VACF  $C_v(t)$ . To this end we solve Eq. (16) with an appropriate initial condition,

$$\mathbf{j}(\mathbf{v}_1, \mathbf{F}; t=0) = \mathbf{v}_1 \quad (17)$$

and then take the first velocity moment of the solution:

$$C_v(t) = \frac{1}{3k_B T} \int d1 d\mathbf{F} f_1^{\text{eq}}(1, \mathbf{F}) \mathbf{v}_1 \cdot \mathbf{j}(\mathbf{v}_1, \mathbf{F}; t). \quad (18)$$

Let us note here, that it follows from Eqs. (16) and (18) that

$$\ddot{C}_v(t=0) = -\omega^2, \quad (19)$$

where  $\omega^2$  is the Einstein frequency:

$$\omega^2 = \frac{1}{3} \text{Tr} \langle \tilde{\Omega}^2 \rangle_F = \frac{n}{3} \int d\mathbf{r} g_2^{\text{eq}}(r) \nabla^2 V(r). \quad (20)$$

$n$  is the density, and  $g_2^{\text{eq}}$  is the pair correlation function. Equation (19) is exact. Thus our theory reproduces the exact short-time behavior of the VACF.

It should be noted here that the binary collision approach results in the following approximate formula:

$$\ddot{C}_v(t=0)|_{bc} = -\frac{n}{3k_B T} \int d\mathbf{r} g_2^{\text{eq}}(r) \nabla V(r) \cdot \nabla V(r). \quad (21)$$

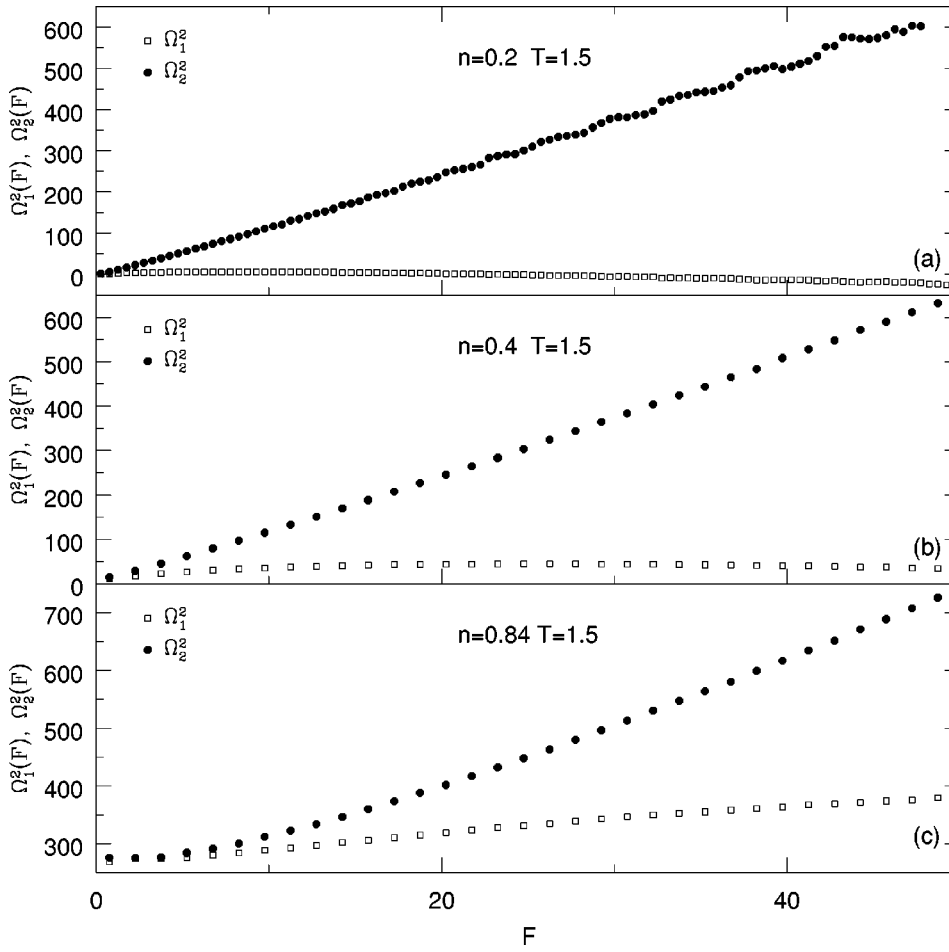


FIG. 4. Two independent elements  $\Omega_1^2$  (empty squares) and  $\Omega_2^2$  (filled circles) of  $\ddot{\Omega}^2$  at  $T=1.5$  and  $n=0.2$  (a),  $n=0.4$  (b) and  $n=0.84$  (c).

It can be shown that the exact formula (19) can be expressed in terms of the total force autocorrelation function,

$$\ddot{C}_v(t=0) = -\frac{1}{3k_B T} G_F(t=0), \quad (22)$$

whereas the approximate formula (21) is related to  $G_F^s$ ,

$$\ddot{C}_v(t=0)|_{bc} = -\frac{1}{3k_B T} G_F^s(t=0). \quad (23)$$

It follows from Fig. 2 and Table I that the binary collision expression (21) greatly overestimates the second derivative of VACF at liquid densities.

Furthermore, Eqs. (16) and (18) lead to the following approximate relation:

$$\begin{aligned} \ddot{C}_v(t=0)|_{th} &= \frac{1}{3} \langle \ddot{\Omega}^2 : \ddot{\Omega}^2 \rangle_F \\ &+ \frac{1}{3k_B T} \int d1 d2 d\mathbf{F} \mathbf{B}_{12} \cdot \mathbf{B}_{12} f_2^{eq}. \end{aligned} \quad (24)$$

Using exact equilibrium distributions obtained from MD simulations (see Appendix C) we have calculated values of the fourth derivative for a liquid with an  $r^{-12}$  interaction for the three states shown in Figs. 1 and 2. We have compared our approximate results with the exact ones. The latter can be obtained by evaluating the exact expression for the fourth derivative through a MD simulation:

$$\ddot{C}_v(t=0) = \frac{1}{3k_B T} \langle \ddot{\mathbf{v}}_1 \cdot \ddot{\mathbf{v}}_1 \rangle_{eq}. \quad (25)$$

Thus, unlike the binary collision approach, our theory predicts the second time derivative of the VACF exactly, and, as Table I shows, gives the fourth time derivative with the accuracy of about 20%.

#### IV. NONDISSIPATIVE DYNAMICS: CAGE OSCILLATIONS

The goal of this paper is to describe the simplest dissipative process: self-diffusion. Before addressing our goal in this section we discuss a nondissipative approximation to the full evolution equation (16),

$$\frac{\partial y_1}{\partial t} = \hat{L}_0 y_1. \quad (26)$$

The motivation for doing this is as follows. In the INM approach<sup>17</sup> one is plagued with negative eigenvalues of the instantaneous matrix of the second derivatives. These give rise to unstable harmonic modes that lead to qualitatively incorrect answers for a variety of physically interesting questions. The most common approach to this problem is to neglect the unstable modes. Neglecting the unstable modes gives rather accurate results. The reasons for this fact are not fully understood.

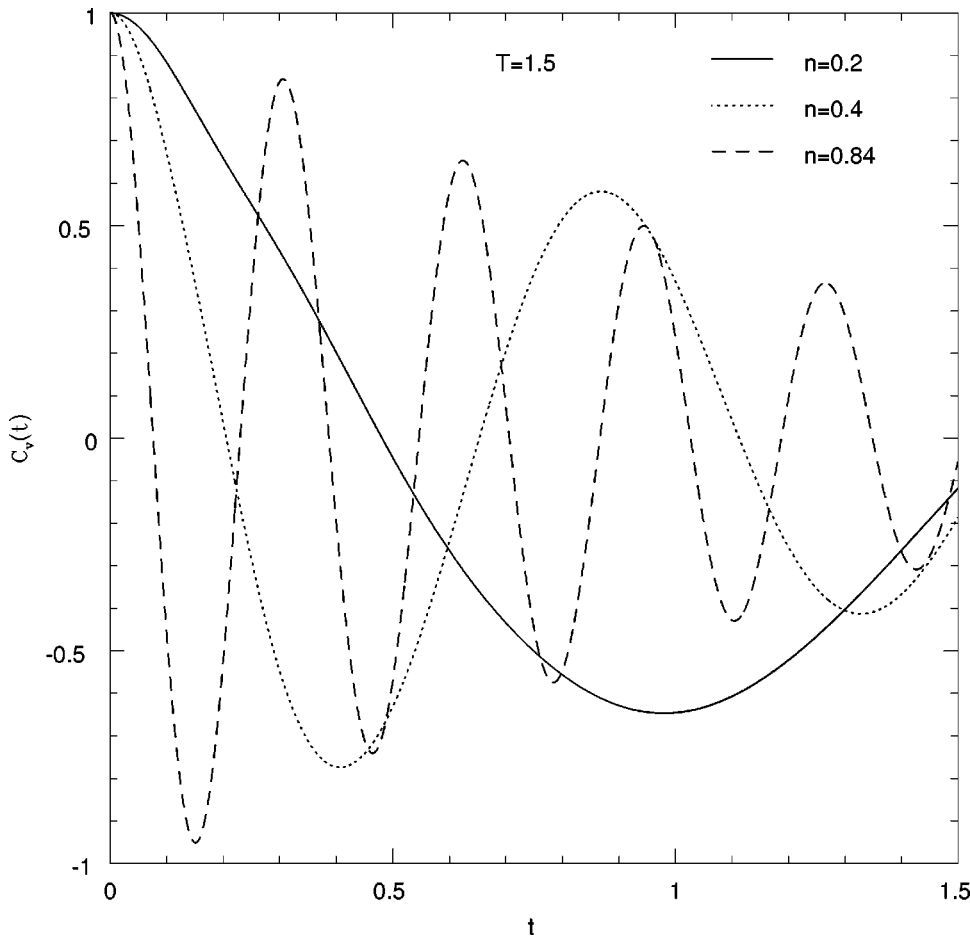


FIG. 5. Velocity autocorrelation functions, obtained in the nondissipative approximation, at  $T=1.5$  and  $n=0.2$  (solid line),  $n=0.4$  (dotted line) and  $n=0.84$  (dashed line).

It turns out that our local matrix of second derivatives,  $\tilde{\Omega}^2$ , also has negative eigenvalues, at least at low densities. Of course,  $\tilde{\Omega}^2$  is positive definite on average (as is the INM-derived matrix of second derivatives),

$$\text{Tr}\langle\tilde{\Omega}^2\rangle_F = \frac{1}{3k_B T} \langle F^2 \rangle_F \geq 0, \quad (27)$$

but this does not guarantee that, say, VACF will not diverge after a relatively short time.

Fortunately, there is the second difference between our nondissipative approximation and the INM approach: our instantaneous matrix  $\tilde{\Omega}^2$  depends on the total force acting on the tagged particle,  $\mathbf{F}$ . This force is changing with time, see Eq. (13c), and therefore the matrix  $\tilde{\Omega}^2$  and the instantaneous frequencies are changing as well. Thus it is possible that the VACF is qualitatively (but not necessarily quantitatively) reasonable even though at some values of  $\mathbf{F}$  the matrix  $\tilde{\Omega}^2$  has negative eigenvalues.

Figures 3 and 4 show the equilibrium distribution of the total force acting on the tagged particle,  $\Psi(\mathbf{F})$ ,

$$\Psi(\mathbf{F}) = \int d1 f_1^{\text{eq}}(\mathbf{r}_1, \mathbf{v}_1, \mathbf{F}), \quad (28)$$

and the two independent elements of the matrix  $\tilde{\Omega}^2$ ,  $\Omega_1^2$  and  $\Omega_2^2$ , are defined as

$$\Omega_{ij}^2 = \frac{F_i F_j}{F^2} \Omega_1^2(F) + \left( \delta_{ij} - \frac{F_i F_j}{F^2} \right) \Omega_2^2(F). \quad (29)$$

$F$  is the magnitude of  $\mathbf{F}$  and  $\Omega_1^2$ , and  $\Omega_2^2$  depend on  $F$  only. For details of MD simulations used to obtain these data, see Appendix C.

It can be seen in Fig. 4 that at low densities and at large enough values of the total force  $\Omega_2^2$  becomes negative.

The nondissipative evolution equation (26) with the initial condition (17) can be solved by the method of characteristics. The resulting VACF has the following form:

$$C_v(t) = \frac{1}{3k_B T} \int d\mathbf{v}_1 d\mathbf{F} \Psi(\mathbf{F}) \varphi_m(\mathbf{v}_1) \mathbf{v}_1 \cdot \mathbf{v}_1(-t), \quad (30)$$

where  $\varphi_m$  is the Maxwell velocity distribution and  $\mathbf{v}_1(-t)$  is the initial  $\mathbf{v}_1$ , transformed backward in time, according to Eqs. (13a)–(13c). The integration in Eq. (30) is simplified by the fact that form (29) of  $\tilde{\Omega}^2$  guarantees that the trajectory of the tagged particle is confined to the plane defined by  $\mathbf{v}_1$  and  $\mathbf{F}$ , and we are left with three integrals instead of six (over magnitudes of  $\mathbf{v}_1$  and  $\mathbf{F}$ , and the angle between them).

Figure 5 shows the VACF obtained in the nondissipative approximation. At all three state points the VACF is bounded. The comparison with Fig. 1 indicates that, as could have been expected, nondissipative VACF is quantitatively incorrect. We would like to remark here that the VACF that

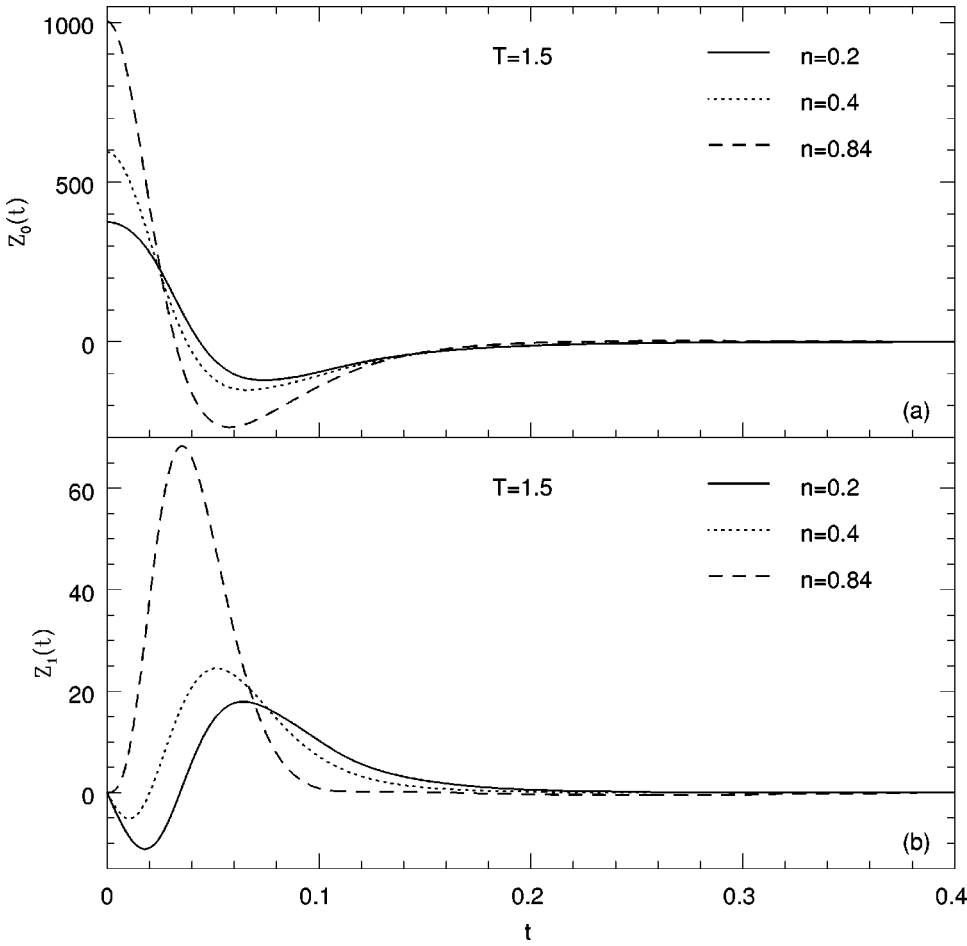


FIG. 6. The collision kernels  $Z_0(t)$  (a),  $Z_1(t)$  (b),  $Z_2(t)$  (c) and  $Z_3(t)$  (d), at  $T=1.5$  and  $n=0.2$  (solid line),  $n=0.4$  (dotted line) and  $n=0.84$  (dashed line).

follows from the nondissipative approximation to the binary collision approach (i.e., from free motion) is time-independent and equal to 1.

## V. DIFFUSION

To calculate  $C_v$  from the full evolution equation (16) we use a moment expansion of  $\mathbf{j}$  that is analogous to the Sonine polynomial expansion used in kinetic theory [see, e.g., Ref. 9, Eq. (4.3)]. The important difference from the kinetic-theory-type expansion is that here the base functions depend on both  $\mathbf{v}_1$  and  $\mathbf{F}$ ,

$$\mathbf{j}(\mathbf{v}_1, \mathbf{F}; t) = C_v(t) \mathbf{v}_1 + B_v(t) \frac{\mathbf{F}}{\omega^2} + A_v(t) \frac{\tilde{\Omega}^2(\mathbf{F}) - \tilde{I} \omega^2}{\gamma \omega^4} \cdot \mathbf{v}_1, \quad (31)$$

where

$$\gamma = \frac{1}{3\omega^4} \langle \tilde{\Omega}^2 : \tilde{\Omega}^2 \rangle_F - 1. \quad (32)$$

As explained in Appendix B this particular form of the moment expansion is motivated by the short time behavior of the VACF.

The (time-dependent) coefficients in the above expansion have the following interpretation:  $C_v$  is the VACF,  $B_v$  is the force-velocity correlation function, and  $A_v$  is the correlation function between  $(\tilde{\Omega}^2(\mathbf{F}) - \tilde{I} \omega^2) \cdot \mathbf{v}_1$  and velocity.

Using ansatz (31) we can relatively easily obtain a closed system of equations for  $A_v, B_v$  and  $C_v$ :

$$\dot{C}_v = B_v, \quad (33)$$

$$\begin{aligned} \dot{B}_v = & -\omega^2 C_v - A_v - \int_0^t d\tau Z_0(\tau) B_v(t-\tau) \\ & - \int_0^t d\tau Z_1(\tau) A_v(t-\tau), \end{aligned} \quad (34)$$

$$\dot{A}_v = \gamma \omega^2 B_v - \int_0^t d\tau Z_2(\tau) B_v(t-\tau) - \int_0^t d\tau Z_3(\tau) A_v(t-\tau), \quad (35)$$

with the initial conditions

$$C_v(t=0) = 1; \quad B_v(t=0) = 0; \quad A_v(t=0) = 0. \quad (36)$$

At  $t=0$  the above equations reproduce Eqs. (19) and (24). Thus the moment expansion preserves the short-time behavior of the VACF.

The collision kernels  $Z_0, Z_1, Z_2$ , and  $Z_3$  are given by the following formulas:

$$Z_0(t) = \frac{1}{3k_B T \omega^2} \int d1 d2 d\mathbf{F} \mathbf{B}_{12} \cdot e^{\hat{L}_2 t} f_2^{\text{eq}} \mathbf{B}_{12},$$

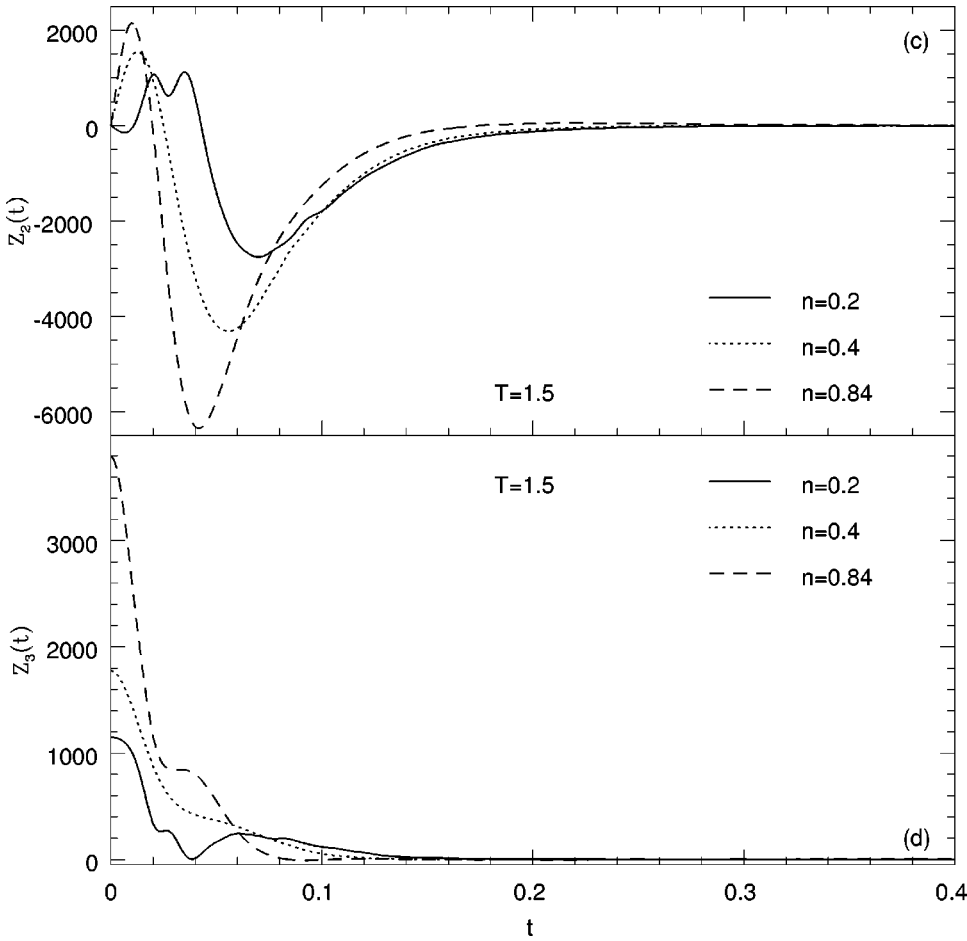


FIG. 6. (Continued.)

$$Z_1(t) = \frac{1}{3k_B T \gamma \omega^4} \int d1 d2 d\mathbf{F} \mathbf{B}_{12} \cdot e^{\hat{L}_2 t} \left( f_2^{\text{eq}} \mathbf{B}_{12} \cdot \frac{\partial}{\partial \mathbf{F}} \right) (\tilde{\Omega}^2 \cdot \mathbf{v}_1),$$

$$Z_2(t) = \frac{1}{3k_B T \omega^2} \int d1 d2 d\mathbf{F} \left( \mathbf{B}_{12} \cdot \frac{\partial}{\partial \mathbf{F}} \right) (\tilde{\Omega}^2 \cdot \mathbf{v}_1) \cdot e^{\hat{L}_2 t} f_2^{\text{eq}} \mathbf{B}_{12},$$

$$Z_3(t) = \frac{1}{3k_B T \gamma \omega^4} \int d1 d2 d\mathbf{F} \left( \mathbf{B}_{12} \cdot \frac{\partial}{\partial \mathbf{F}} \right) (\tilde{\Omega}^2 \cdot \mathbf{v}_1) \cdot e^{\hat{L}_2 t} \left( f_2^{\text{eq}} \mathbf{B}_{12} \cdot \frac{\partial}{\partial \mathbf{F}} \right) (\tilde{\Omega}^2 \cdot \mathbf{v}_1).$$

To calculate the collision kernels one has to solve the two-particle equations of motion, represented by  $\hat{L}_2$  (8). In

our case, these equations describe the motion of two particles interacting via the potential  $V(r)$  in the presence of a constant external force acting on one of them. In explicit calculations we need the equilibrium distribution  $f_2^{\text{eq}}(\mathbf{r}_1 - \mathbf{r}_2, \mathbf{F})$  that we obtain from the MD simulations. We would like to emphasize that the theory uses as input only *equilibrium* information about the liquid.

To evaluate, e.g.,  $Z_0(t)$  we write it as  $Z_0(t) \propto \int \mathbf{B}_{12}(t) f_2^{\text{eq}} \mathbf{B}_{12}$  where  $\mathbf{B}_{12}(t)$  denotes  $\mathbf{B}_{12}$  transformed forward in time according to the two-particle equations of motion represented by  $\hat{L}_2$ . The remaining integral is evaluated numerically at each subsequent time. To this end we use the VEGAS algorithm, which performs Monte Carlo integration based on importance sampling.<sup>27</sup> Figure 6 shows  $Z_i, i = 0, 1, 2, 3$  for three different state points.

The equations of motion for  $A_v, B_v$  and  $C_v$  can be solved by using a Fourier-Laplace transform,  $\tilde{f}(p) = \int_0^\infty dt e^{ipt} f(t)$ . The transform of the VACF is

$$\tilde{C}_v(p) = \left( \frac{\omega^2}{-ip + \tilde{Z}_0(p) + (1 + \tilde{Z}_1(p))(\gamma \omega^2 - \tilde{Z}_2(p)) / (-ip + \tilde{Z}_3(p))} - ip \right)^{-1}. \tag{37}$$

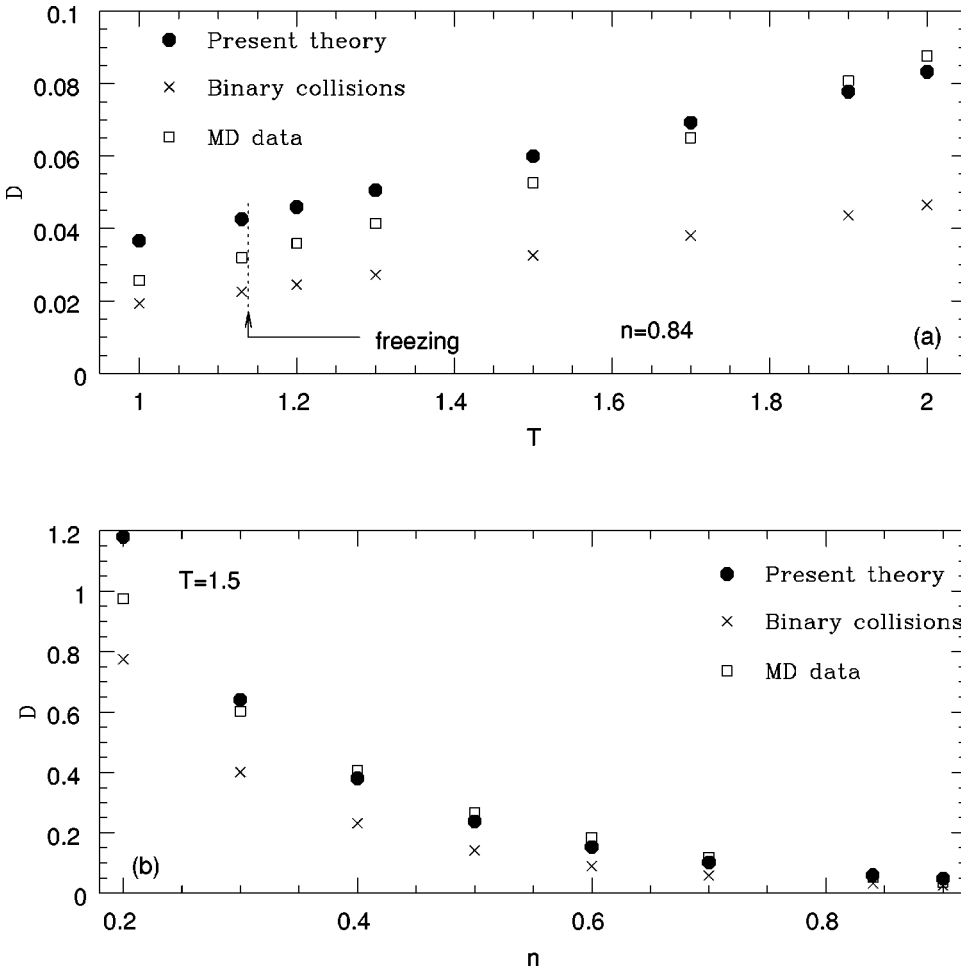


FIG. 7. The self-diffusion coefficient as a function of temperature at  $n = 0.84$  (a) and as a function of density at  $T = 1.5$  (b). Filled circles, present theory; crosses, results of the binary collisions calculations based on the theory of Refs. 8 and 9; squares, results of MD simulations.

The VACF in the time domain is obtained by applying an inverse transform to Eq. (37).

It is easy to obtain the Fourier-Laplace transform of the memory function  $\tilde{\zeta}(p)$ , defined through the equation:

$$\dot{C}_v(t) = - \int_0^t d\tau \zeta(\tau) C_v(t - \tau), \quad (38)$$

or, after performing a Fourier-Laplace transform,

$$\tilde{C}_v(p) = (\tilde{\zeta}(p) - ip)^{-1}. \quad (39)$$

Thus, given Eq. (37), the Fourier-Laplace transform of the memory function reads

$$\tilde{\zeta}(p) = \frac{\omega^2}{-ip + \tilde{Z}_0(p) + (1 + \tilde{Z}_1(p))(\gamma\omega^2 - \tilde{Z}_2(p)) / (-ip + \tilde{Z}_3(p))}. \quad (40)$$

Finally, the self-diffusion coefficient is given by the following expression:

$$D = k_B T \tilde{C}_v(0) = k_B T \left( \frac{\tilde{Z}_0(0)}{\omega^2} + (1 + \tilde{Z}_1(0)) \frac{\gamma - \tilde{Z}_2(0)/\omega^2}{\tilde{Z}_3(0)} \right). \quad (41)$$

## VI. COMPARISON WITH MD

Theoretical predictions are compared to the self-diffusion coefficient and the VACF obtained from the same MD simulations, as  $f_2^{\text{eq}}$ . In Fig. 7 we show the temperature dependence of the self-diffusion coefficient at constant density and the density dependence at constant temperature. In both cases we get quantitative agreement between the theory and simulations.

In our system the energy and length scales of the poten-

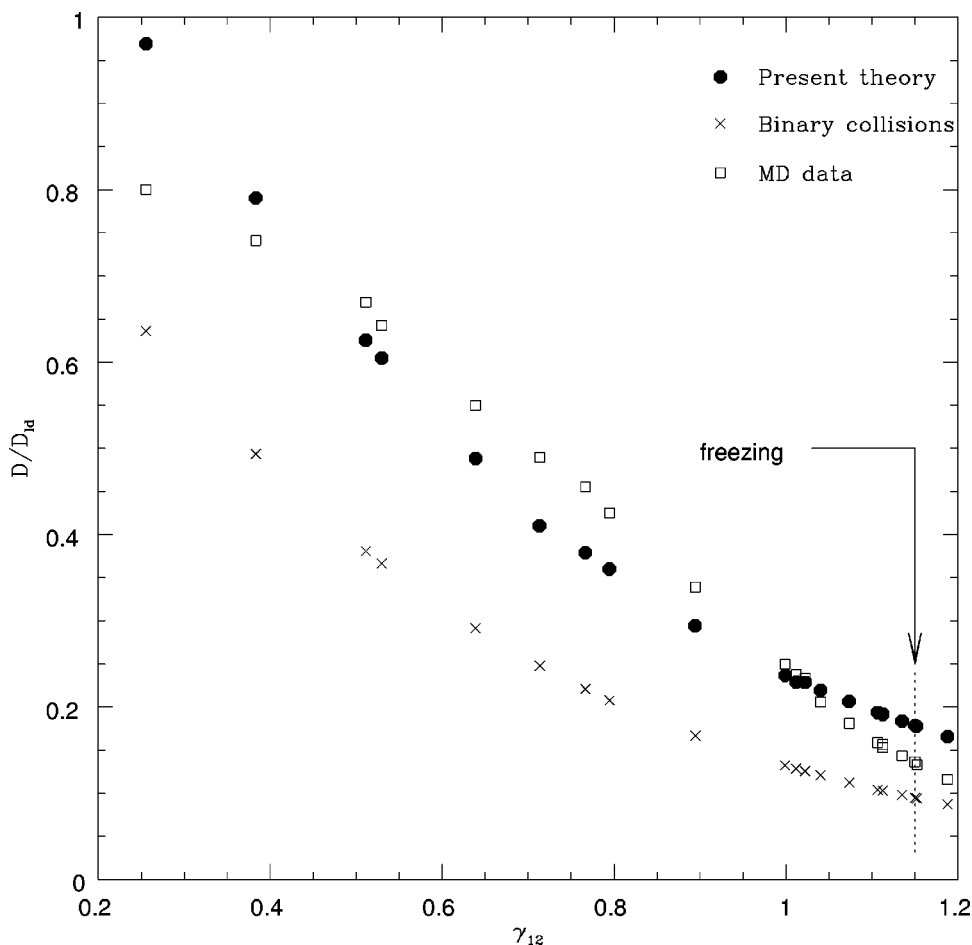


FIG. 8. Diffusion coefficient, scaled by its low density value  $D_{ld}$ , as a function of the dimensionless coupling constant  $\gamma_{12}$ . Filled circles, present theory; crosses, results of the binary collisions calculations based on the theory of Refs. 8 and 9; squares, results of MD simulations.

tial are not independent: the potential depends only on a certain combination of  $\epsilon$  and  $\sigma$  ( $\epsilon\sigma^{12}$ ). Thus, the state of the system is uniquely determined by the value of a single dimensionless parameter<sup>28</sup>  $\gamma_{12} = n\sigma^3(4\epsilon/k_B T)^{1/4}$ . All quantities can be scaled in such a way that they depend only on the value of  $\gamma_{12}$  and not on temperature or density separately. For instance, the diffusion coefficient should be scaled by its low-density value:<sup>26</sup>

$$D_{ld} = 0.234 \left( \frac{k_B T}{m} \right)^{1/2} \left( \frac{k_B T}{4\epsilon} \right)^{1/6} \frac{1}{n\sigma^2}. \quad (42)$$

Figure 8 shows the diffusion coefficient, scaled by its low-density value  $D_{ld}$ , as a function of  $\gamma_{12}$ . One can see that our theoretical predictions are in good agreement with the MD results.

Figure 9 presents a comparison between VACF obtained in MD simulations, and the results of our calculations. Our theory, by construction, gives the correct short-time behavior of the VACF. We are also able to reproduce all essential qualitative features of the VACF and to reach a good overall agreement with MD simulations.

Finally, in Fig. 10 we compare the memory function<sup>25</sup>  $\zeta(t)$  obtained from MD simulations (for a detailed procedure used to extract the memory function, see Appendix C) and the predictions of our theory. Our approach, by construction, reproduces exactly  $\zeta(t=0)$ . We are also correctly describing the short-time dependence of the memory function. In par-

ticular, the second time derivative of  $\zeta(t)$  at  $t=0$  is reproduced quantitatively (within 20%). Qualitatively, our theory does not reproduce the long time features in the memory function that are typically explained in terms of dynamic correlations.

## VII. CONCLUSIONS

We presented here an alternative approach to self-diffusion in liquids. The theory requires only *equilibrium* information about the liquid. It uses the oscillatory motion of a tagged particle in a cage, made by the first solvation shell, as the zeroth order approximation. The theory predicts the self-diffusion coefficient, VACF and the memory function which quantitatively agree with the results of MD simulations in a broad range of temperatures and densities up to the freezing transition.

Our theory can be extended in several ways. First, we would like to describe single-molecule processes of chemical importance such as solvation and vibrational relaxation in nonpolar liquids. At present we are working on a modification of the formalism that would allow us to calculate the dynamic friction on the intermolecular bond.<sup>4</sup> Second, we would like to extend the present theory to ‘‘collective’’

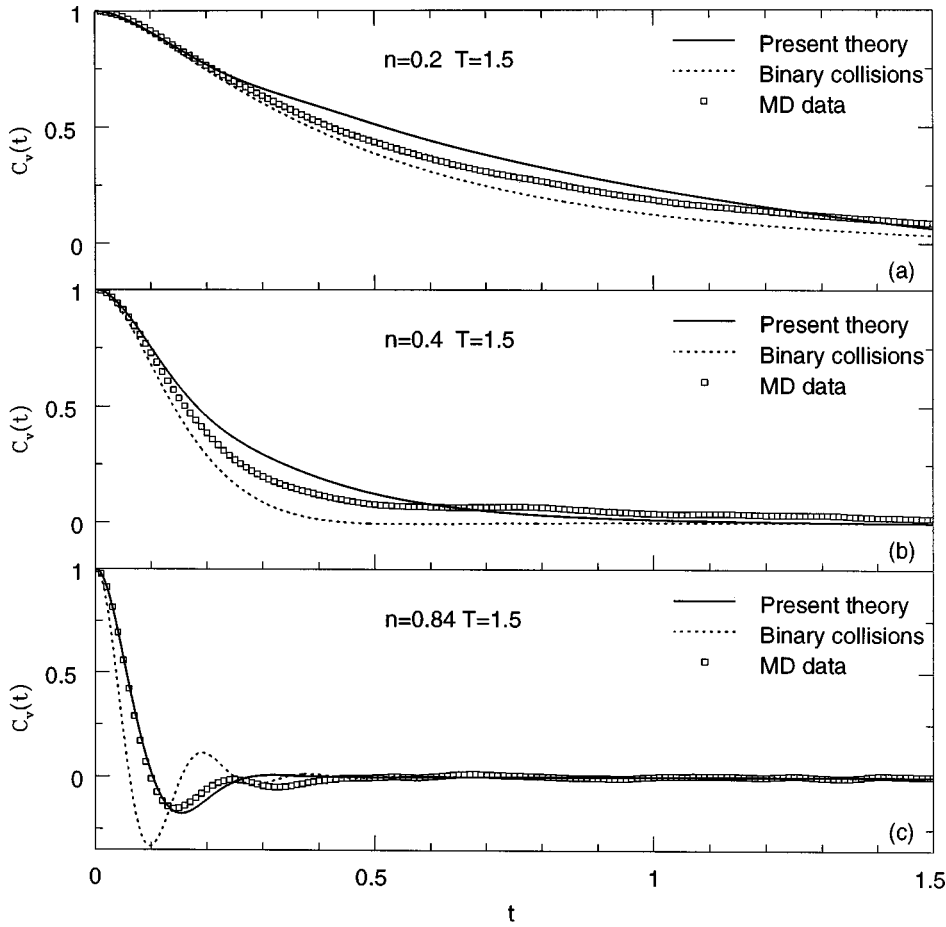


FIG. 9. VACF at  $T=1.5$  and  $n=0.2$  (a),  $n=0.4$  (b) and  $n=0.84$  (c). Solid lines represent our results; dotted lines, results of the binary collisions calculations based on the theory of Refs. 8 and 9; points, results of MD simulations.

transport phenomena in liquids and the calculation of all the transport coefficients. Finally, the present theory does not include dynamic correlations; we hope that by including these correlations we can get a better agreement with simulations in the supercooled liquid regime.

## ACKNOWLEDGMENTS

Grzegorz Szamel is a Cottrell Scholar of Research Corporation. This work was partially supported by NSF Grant No. CHE-9624596.

## APPENDIX A

To derive Eq. (5) one writes down an expression for the time derivative of  $f_1$ ,

$$\frac{\partial f_1}{\partial t} = \int d\Gamma \delta(\mathbf{r}_1 - \mathbf{R}_1) \delta(\mathbf{v}_1 - \mathbf{V}_1) \delta\left(\mathbf{F} + \frac{\partial}{\partial \mathbf{R}_{1j \neq 1}} V(R_{1j})\right) \times \mathcal{L}_N \rho_N(\Gamma; t), \quad (\text{A1})$$

where

$$\mathcal{L}_N = - \sum_{i=1}^N (\dot{\mathbf{v}}_i \cdot \partial / \partial \mathbf{v}_i + \dot{\mathbf{r}}_i \cdot \partial / \partial \mathbf{r}_i) \quad (\text{A2})$$

is the  $N$ -particle Liouville operator.<sup>25</sup> Then one integrates this expression by parts and uses  $\delta$ -functions to perform the integration. The derivatives of the first two  $\delta$ -functions give

rise to the two first terms in Eq. (5), since  $\dot{\mathbf{r}}_1 = \mathbf{v}_1$  and  $\dot{\mathbf{v}}_1 = \mathbf{F}$ . The last term is more complicated:  $\dot{\mathbf{F}}$  cannot be expressed in terms of 1-particle quantities (similar to  $\dot{\mathbf{v}}_1$  in the standard BBGKY), and therefore involves  $f_2$  (the last term in Eq. (5)). Derivation of the second equation in the hierarchy is done in a similar fashion.

## APPENDIX B

To show why  $A_v$  and  $B_v$  appear in the moment expansion (31), we calculate the time derivative of  $C_v$  using Eqs. (18) and (16):

$$\begin{aligned} \dot{C}_v &= \frac{1}{3k_B T} \int d1 d\mathbf{F} f_1^{\text{eq}}(1, \mathbf{F}) \mathbf{v}_1 \cdot \hat{L}_0 \mathbf{j}(\mathbf{v}_1, \mathbf{F}; t) \\ &= \frac{1}{3k_B T} \int d1 d\mathbf{F} f_1^{\text{eq}}(1, \mathbf{F}) \mathbf{F} \cdot \mathbf{j}(\mathbf{v}_1, \mathbf{F}; t) \equiv B_v. \end{aligned} \quad (\text{B1})$$

The integral term of Eq. (16) does not contribute to  $\dot{C}_v$ , and we get Eq. (33). Next we calculate the time derivative of  $B_v$ :

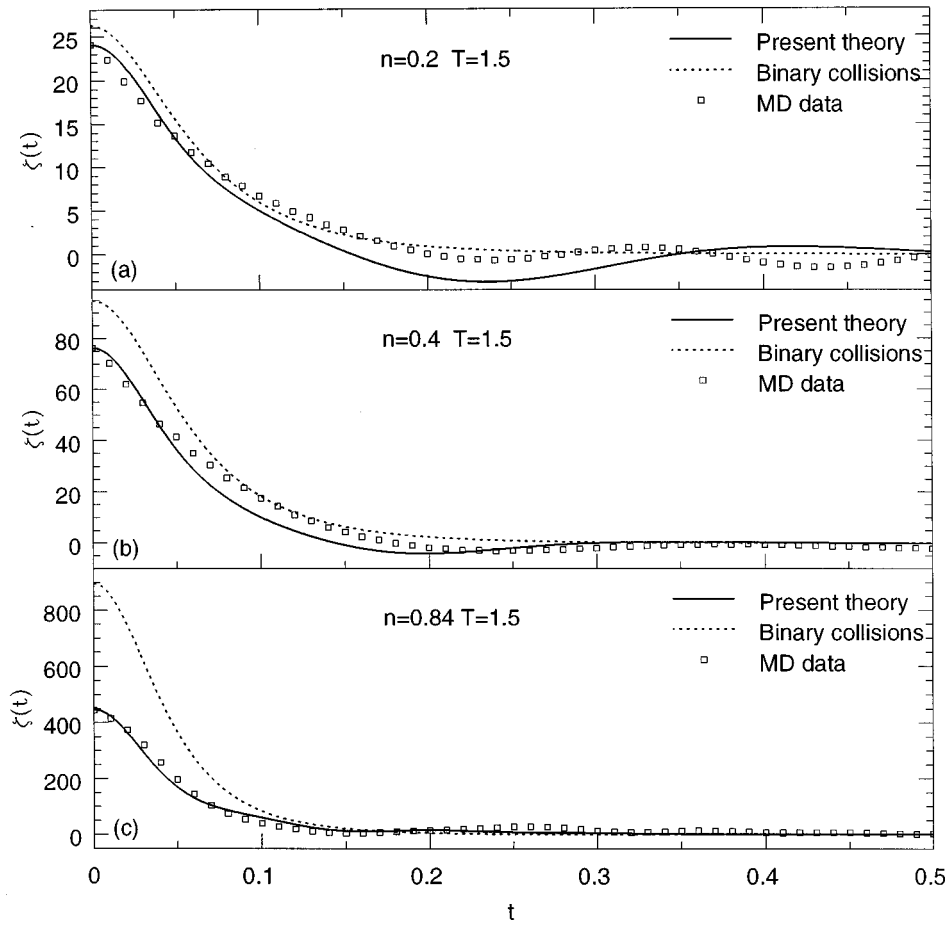


FIG. 10. Memory function  $\zeta(t)$  at  $T = 1.5$  and  $n=0.2$  (a),  $n=0.4$  (b) and  $n=0.84$  (c). Solid lines represent our results; dotted lines, results of the binary collisions calculations based on the theory of Refs. 8 and 9; points, results of MD simulations.

$$\begin{aligned}
 \dot{B}_v &= \frac{1}{3k_B T} \int d1 d\mathbf{F} f_1^{\text{eq}}(1, \mathbf{F}) \mathbf{F} \cdot \hat{L}_0 \mathbf{j}(\mathbf{v}_1, \mathbf{F}; t) \\
 &+ \frac{1}{f_1^{\text{eq}}} \int d2 \mathbf{B}_{12} \cdot \frac{\partial}{\partial \mathbf{F}} \int_0^t d\tau e^{\hat{L}_2(t-\tau)} f_2^{\text{eq}} \mathbf{B}_{12} \cdot \frac{\partial \mathbf{j}(\mathbf{v}_1, \mathbf{F}; \tau)}{\partial \mathbf{F}} \\
 &= -\frac{1}{3k_B T} \int d1 d\mathbf{F} f_1^{\text{eq}}(1, \mathbf{F}) (\tilde{\Omega}^2 \cdot \mathbf{v}_1) \cdot \mathbf{j}(\mathbf{v}_1, \mathbf{F}; t) \\
 &+ \frac{1}{f_1^{\text{eq}}} \int d2 \mathbf{B}_{12} \cdot \frac{\partial}{\partial \mathbf{F}} \int_0^t d\tau e^{\hat{L}_2(t-\tau)} f_2^{\text{eq}} \mathbf{B}_{12} \cdot \frac{\partial \mathbf{j}(\mathbf{v}_1, \mathbf{F}; \tau)}{\partial \mathbf{F}} \\
 &= -\omega^2 C_v - \frac{1}{3k_B T} \int d1 d\mathbf{F} f_1^{\text{eq}}(1, \mathbf{F}) ((\tilde{\Omega}^2 - \tilde{I} \omega^2) \cdot \mathbf{v}_1) \\
 &\cdot \mathbf{j}(\mathbf{v}_1, \mathbf{F}; t) + \frac{1}{f_1^{\text{eq}}} \int d2 \mathbf{B}_{12} \cdot \frac{\partial}{\partial \mathbf{F}} \int_0^t d\tau e^{\hat{L}_2(t-\tau)} f_2^{\text{eq}} \mathbf{B}_{12} \\
 &\cdot \frac{\partial \mathbf{j}(\mathbf{v}_1, \mathbf{F}; \tau)}{\partial \mathbf{F}} \\
 &\equiv -\omega^2 C_v - A_v + \frac{1}{f_1^{\text{eq}}} \int d2 \mathbf{B}_{12} \\
 &\cdot \frac{\partial}{\partial \mathbf{F}} \int_0^t d\tau e^{\hat{L}_2(t-\tau)} f_2^{\text{eq}} \mathbf{B}_{12} \cdot \frac{\partial \mathbf{j}(\mathbf{v}_1, \mathbf{F}; \tau)}{\partial \mathbf{F}}. \tag{B2}
 \end{aligned}$$

At short times, the contribution of the integral term is negligible, and we are left with

$$\dot{B}_v = -\omega^2 C_v - A_v. \tag{B3}$$

Thus, ansatz (31) allows us to describe the short-time behavior of the VACF exactly. Note that we are using ansatz (31) for all times and this constitutes another approximation. It should be relatively straightforward to improve upon Eq. (31) by adding additional terms. This is left for a future study.

To get Eqs. (B1) and (B2) we performed integration by parts and used the fact that  $f_1^{\text{eq}}$  satisfies the equation:

$$\mathbf{v}_1 \cdot \frac{\partial f_1^{\text{eq}}}{\partial \mathbf{r}_1} + \mathbf{F} \cdot \frac{\partial f_1^{\text{eq}}}{\partial \mathbf{v}_1} = \frac{\partial}{\partial \mathbf{F}} (f_1^{\text{eq}} \tilde{\Omega}^2 \cdot \mathbf{v}_1), \tag{B4}$$

following from Eq. (5) and the definition of  $\tilde{\Omega}^2$  (12).

### APPENDIX C

All explicit calculations in this work are done using the following model system:  $N = 1372$  particles interacting via a pairwise potential

$$V(r) = 4\epsilon(\sigma/r)^{12}. \tag{C1}$$

This potential is a repulsive part of the well-known Lennard-Jones potential  $V_{\text{LJ}}(r) = 4\epsilon((\sigma/r)^{12} - (\sigma/r)^6)$ , which with  $\sigma = 3.4 \text{ \AA}$  and  $\epsilon/k_B = 120 \text{ K}$ , along with molecular mass  $m = 40 \text{ a.u.}$ , is known to successfully reproduce the properties of liquid argon.<sup>14</sup> The natural time unit is then given by  $\tau = \sigma\sqrt{m/\epsilon} = 2.16 \times 10^{-12} \text{ s}$ . All dimensional quantities in this

paper given as pure numbers should be understood as multiplied by an appropriate combination of  $\sigma, \epsilon$  and  $m$  (MD units).

We have used a standard, fifth order predictor-corrector algorithm with a time step of  $0.0025\tau$  in our simulations. Periodic boundary conditions were imposed on the system in all three directions.

From MD simulations we obtained (1)  $f_2^{\text{eq}}$ , which was used in our theoretical calculations, and (2) the self-diffusion coefficient, VACF and the memory function, against which we checked our results.

While the self-diffusion coefficient and VACF are straightforward to obtain from the MD data, it is well known that obtaining the memory function is more involved. We used two methods to get the memory function: first, we applied a discrete Fourier transform to the VACF, using Eq. (39) obtained a Fourier transform of the memory function and then, by applying an inverse discrete Fourier transform obtained the memory function in the time domain, which was subsequently smoothed to remove spurious oscillations. Second, we iteratively solved Eq. (38) for the memory function. At high densities, these two methods give essentially the same results, but at low densities the second method becomes unstable.

<sup>1</sup>B. Bagchi, *Annu. Rev. Phys. Chem.* **40**, 115 (1989); M. J. Maroncelli, *J. Mol. Liq.* **57**, 1 (1993), and references therein.

<sup>2</sup>B. M. Ladanyi and R. M. Stratt, *J. Phys. Chem.* **99**, 2502 (1995); **100**, 1266 (1996).

<sup>3</sup>C. B. Harris, D. E. Smith, and D. J. Russel, *Chem. Rev.* **90**, 481 (1990).

<sup>4</sup>B. J. Berne, M. E. Tuckerman, J. E. Straub, and A. L. R. Bug, *J. Chem. Phys.* **93**, 5084 (1990); G. Goodyear, R. E. Larsen, and R. M. Stratt, *Phys. Rev. Lett.* **76**, 243 (1996); G. Goodyear and R. M. Stratt, *J. Chem. Phys.* **105**, 10050 (1996).

<sup>5</sup>H. G. Hertz, *Ber. Bunsenges. Phys. Chem.* **77**, 531 (1973); J. T. Hynes and P.G. Wolynes, *J. Chem. Phys.* **75**, 395 (1981).

<sup>6</sup>E. G. D. Cohen, *Am. J. Phys.* **61**, 524 (1993).

<sup>7</sup>E. G. D. Cohen, *Physica A* **194**, 229 (1993).

<sup>8</sup>S. Ranganathan, *Can. J. Phys.* **61**, 1655 (1983).

<sup>9</sup>J. A. Leegwater, *J. Chem. Phys.* **94**, 7402 (1991).

<sup>10</sup>J. R. Dorfman and E. G. D. Cohen, *Phys. Rev. Lett.* **25**, 1257 (1972).

<sup>11</sup>P. Résibois, *J. Stat. Phys.* **13**, 393 (1975).

<sup>12</sup>M. H. Ernst, E. H. Hauge, and J. M. J. van Leeuwen, *Phys. Rev. Lett.* **25**, 1254 (1972).

<sup>13</sup>J.-P. Hansen and I. R. McDonald, *Theory of Simple Liquids* (Academic, London, 1990).

<sup>14</sup>L. Sjögren and A. Sölander, *J. Phys. C* **12**, 4396 (1979); L. Sjögren, *ibid.* **13**, 705 (1980).

<sup>15</sup>K. Kim and D. Chandler, *J. Chem. Phys.* **59**, 5215 (1973).

<sup>16</sup>R. Zwanzig, *J. Chem. Phys.* **79**, 4507 (1983).

<sup>17</sup>T. Keyes, *J. Phys. Chem. A* **101**, 2921 (1997).

<sup>18</sup>J. Cao and G. A. Voth, *J. Chem. Phys.* **103**, 4211 (1995).

<sup>19</sup>E. Rabani, J. D. Gezelter, and B. J. Berne, *J. Chem. Phys.* **107**, 6867 (1997).

<sup>20</sup>M. Buchner, B. M. Ladanyi, and R. M. Stratt, *J. Chem. Phys.* **97**, 8522 (1992); M. Cho *et al.*, *ibid.* **100**, 6672 (1994).

<sup>21</sup>T. Keyes, *J. Chem. Phys.* **101**, 5081 (1994); **103**, 9810 (1995).

<sup>22</sup>J. D. Gezelter, E. Rabani, and B. J. Berne, *J. Chem. Phys.* **107**, 4618 (1997).

<sup>23</sup>See also, T. Keyes, W.-X. Li, and U. Zurcher, *J. Chem. Phys.* **109**, 4693 (1998); J. D. Gezelter, E. Rabani, and B. J. Berne, *ibid.* **109**, 4695 (1998).

<sup>24</sup>Interestingly, the first part of our program has been applied to a hard sphere fluid by Tang and Evans [ *Phys. Rev. Lett.* **72**, 1666 (1994)]. These authors used a harmonic mode model for self-diffusion; for high densities their VACF agrees well with the MD data; they did not include cage relaxation and therefore could not calculate the self-diffusion coefficient. Harmonic motion has also been invoked in a study of the hard sphere crystal dynamics [ T. Kirkpatrick, *J. Stat. Phys.* **57**, 483 (1989)].

<sup>25</sup>B. J. Berne and G. D. Harp, *Adv. Chem. Phys.* **17**, 63 (1970).

<sup>26</sup>P. Résibois and M. De Leener, *Classical Kinetic Theory of Fluids* (Wiley, New York, 1977).

<sup>27</sup>G. P. Lepage, *J. Comput. Phys.* **27**, 192 (1978); W. H. Press, S. A. Teukolsky, W. T. Vetterling, and B. P. Flannery, *Numerical Recipes in FORTRAN*, 2nd ed. (Cambridge University Press, New York, 1992).

<sup>28</sup>B. B. Laird and D. M. Kroll, *Phys. Rev. A* **42**, 4810 (1990).